istics was estimated by means of a comparison of the modified model with the original Pao–Sah model [1].

The relative error of "uniform" models decreases with gate voltage and increases with drain-to-source voltage and source-to-bulk voltage.

The influence of nonuniform doping profile diminishes when the oxide thickness is decreased even if the reduction of gate-oxide thickness is accompanied by a corresponding increase of substrate doping concentration.

If the box width is increased the accuracy of the uniform model assuming bulk doping improves, while that of the model assuming surface doping worsens.

In most cases the error of approximation of the box profile assuming uniform doping equal to N_{surf} is less than 1%.

REFERENCES

[1] H. C. Pao and C. T. Sah, "Effects of diffusion current on characteristics of metal-oxide (insulator)-semiconductor transistors," *Solid-State Electron.*, vol. 9, pp. 927–937, 1966.
[2] J. R. Brews, W. Fichtner, E. Nicollian, and S. M. Sze, "Generalized guide for MOSFET miniaturization," in *IEDM Tech. Dig.*, 1979, pp. 10–13, and *IEEE Electron Device Lett.*, vol. EDL-1, pp. 2–4, 1980.
[3] S. Karmalhar and K. N. Bhat, "A process-parameter-based circuit simulation model for ion-implanted MOSFET's," *IEEE J. Solid State Circuits*, vol. 24, no. 1, pp. 139–145, 1989.
[4] D. M. Rogers, J. D. Hayden, and D. D. Rinerson, "Model for the channel-implanted enhancement mode IGFET," *IEEE Trans. Electron Devices*, vol. ED-33, no. 7, pp. 955–964, 1986.
[5] R. H. Kingston and S. F. Neustadter, "Calculation of the space-charge, electric field and free carrier concentration at the surface of a semiconductor," *J. Appl. Phys.*, vol. 26, pp. 718–720, 1955.

Hydrodynamic and Monte Carlo Simulation of an Electron Shock Wave in a 1-μm n^+-n-n^+ Diode

Carl L. Gardner

***Abstract*—Hydrodynamic model simulations of a steady-state electron shock wave in a 1-μm Si semiconductor device at 77 K are compared with a Monte Carlo simulation of the Boltzmann equation using the DAMOCLES program. Excellent agreement between the two different methods for simulating the electron shock wave can be obtained by adjusting the amount of heat conduction in the hydrodynamic model.**

I. INTRODUCTION

In [1], two parameter regimes for the n^+-n-n^+ diode are presented in which a shock profile develops in the channel as the supersonic flow on entering the channel breaks to a subsonic flow, in analogy with gas dynamical flow in a Laval nozzle. The electron shock wave is a new nonlinear wave analogous to the gas dynamical shock wave in the Laval nozzle, but in a very different physical setting. Here the n^+-n-n^+ doping of the diode corresponds to the converging/diverging geometry of the Laval nozzle.

The steady-state upwind shock simulations presented in [1] were reproduced in [2] using a time-dependent "essentially nonoscillatory" (ENO) upwind scheme, a higher order Godunov method.

The shock computations imply that the electron shock waves are an integral part of the hydrodynamic model. The shock waves allow higher electron velocities to develop in the diode channel, and provide a richer space-charge structure in the diode channel.

In [3], numerical simulations of a family of steady-state electron shock waves (parametrized by the amount of heat conduction) in a 1-μm Si semiconductor device at 77 K were presented. The electron shock wave has a finite width which scales linearly with the amount of heat conduction. Numerical evidence was given that the shock width goes to zero as the amount of heat conduction in the model goes to zero.

Manuscript received June 17, 1992; revised September 11, 1992. This research was supported in part by the Army Research Office under Grant DAAL03-91-G-0146. The review of this brief was arranged by Associate Editor A. H. Marshak.

The author is with the Department of Computer Science and the Department of Mathematics, Duke University, Durham, NC 27706.

IEEE Log Number 9205178.

II. COMPARISON OF HYDRODYNAMIC AND MONTE CARLO COMPUTATIONS

In this section, I present the confirmation of the original prediction of the 77 K electron shock wave in Si by a Monte Carlo simulation of Laux of the Boltzmann equation using the DAMOCLES [4] program. For the shock computations, I take an n^+-n-n^+ diode with n^+ doping density $N = 10^{18}$ cm^{-3} and n doping density $N = 10^{15}$ cm^{-3}.

I use modified Baccarani–Wordemann models [5], [3] for the momentum and energy relaxation times in the hydrodynamic model

$$\tau_p = \frac{\tau_{p0}}{1 + (N/N_{ref})^{\alpha}} \frac{T_0}{T} \tag{1}$$

$$\tau_w = \frac{\tau_p}{2}\left(1 + \frac{\frac{3}{2}T}{\frac{1}{2}mv_s^2}\right) \tag{2}$$

where the low-energy momentum relaxation time τ_{p0} is set equal to 1.67 ps from the DAMOCLES data [6] for 0.00995 eV electrons[1] in homogeneous Si, N is the doping density, T is the electron temperature, T_0 is the ambient device temperature, m is the effective electron mass, and $v_s = v_s(T_0)$ is the saturation velocity. For Si at 77 K, $N_{ref} = 1.44 \times 10^{15}$ cm^{-3}, $\alpha = 0.659$, $m = 0.24m_e$, and $v_s = 1.2 \times 10^7$ cm/s.

Excellent agreement between the two different methods for simulating the electron shock wave can be obtained by adjusting the amount of heat conduction in the hydrodynamic model. The best fit for the thermal conductivity κ in the law for heat conduction

$$\boldsymbol{q} = -\kappa \nabla T, \qquad \kappa \approx \kappa_0 \tau_{p0} n T_0 / m \tag{3}$$

where n is the electron density, is given by $\kappa_0 = 0.05$.

Figs. 1 and 2 present the hydrodynamic and DAMOCLES simulations of the 77 K electron shock wave in Si at a bias $V = 1$ V. The diode consists of a 0.1-μm source, a 1.0-μm channel, and a 0.1-μm drain. DAMOCLES calculates a current of 4500 A/cm^2, in agreement with the hydrodynamic value of 4460 A/cm^2. The shock profile is most clearly visible in the velocity plot Fig. 1 (the electrons flow from left to right). The flow is supersonic at the velocity peak just inside the channel, and subsonic at the end of the wave where the velocity makes a "bend" to the plateau in the channel.

[1] The equilibrium electron average energy at 77 K.

0018-9383/93$03.00 © 1993 IEEE

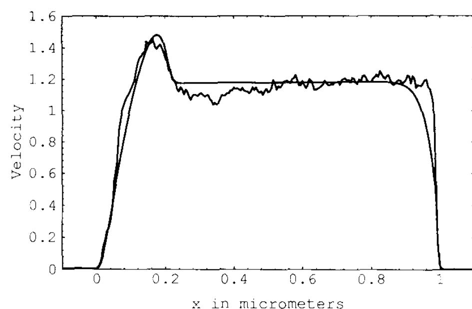

Fig. 1. Hydrodynamic and Monte Carlo electron velocity in 10^7 cm/s for $V = 1$ V, 1-μm channel, 77 K Si. The jagged curve is the DAMOCLES result. The channel is between $x = 0$ and $x = 1$ μm.

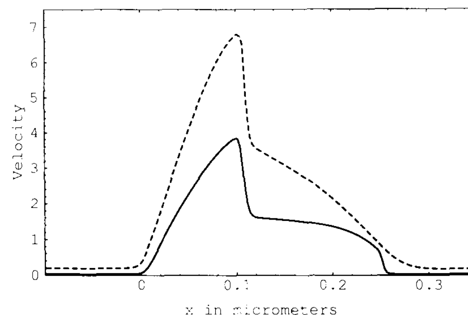

Fig. 3. Hydrodynamic electron velocity in 10^7 cm/s for $V = 1$ V, 0.25-μm channel, 77 K Si and 300 K GaAs (dotted curve). The channel is between $x = 0$ and $x = 0.25$ μm.

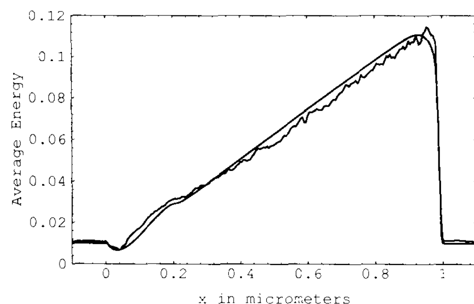

Fig. 2. Hydrodynamic and Monte Carlo electron average energy in electronvolts for $V = 1$ V, 1-μm channel, 77 K Si. The jagged curve is the DAMOCLES result.

The DAMOCLES velocity exhibits a Mach 2.1 shock profile (slightly spread out due to heat conduction) based on both internal evidence[2] and comparison with the hydrodynamic simulations. Thus the hydrodynamic prediction of an electron shock wave [1] in Si at 77 K has been confirmed by Monte Carlo simulation of the Boltzmann equation.

The electron shock waves presented in [1] and [3] were too strong (the peak electron velocities of 2.8 and 1.7×10^7 cm/s, respectively, were too high) because the low-field electron mobilities (21 000 and 18 000 $\text{cm}^2/\text{V} \cdot \text{s}$, respectively) set τ_{p0} too high. The low-field electron mobility μ_{n0} is related to τ_{p0} by $\tau_{p0} = m\mu_{n0}/e$. Setting $\tau_{p0} = 1.67$ ps corresponds to a low-field electron mobility of 12 200 $\text{cm}^2/\text{V} \cdot \text{s}$. While this value is too low to correspond to the experimental values $\approx$ 18 000 $\text{cm}^2/\text{V} \cdot \text{s}$, I believe it is the correct prescription for the hydrodynamic model since we require not the *low-field* momentum relaxation time, but instead the *low-energy* value for electrons with average energy $w_0 = 3T_0/2$.

Stronger shock waves develop in shorter devices. For a 0.25-μm channel device with a 1-V bias, my hydrodynamic code predicts (see Fig. 3) a Mach 4.7 shock in Si at 77 K and a Mach 2.7 shock in GaAs at 300 K.

The type of dramatic velocity overshoot illustrated in Figs. 1 and 3 is always associated with a shock wave (spread out due to heat conduction) for the n^+-n-n^+ diode. As the electrons enter the channel, the electron velocity increases rapidly to a peak value greater than the saturation velocity v_s. At the same time, the electron temperature falls slightly as the electrons overcome the small potential barrier at the source/channel junction. Thus the electron Mach number M near the velocity peak is greater than $v_s/c > v_s/c_0$, where $c = \sqrt{T/m}$ is the sound speed at temperature T and c_0 is the sound speed at the ambient temperature T_0. For Si at 77 K, $v_s = 1.2 \times 10^7$ cm/s, $c_0 = 7.0 \times 10^6$ cm/s, and $M > 1.7$. On the other hand, the electron flow near the channel/drain is subsonic since $v \approx v_s$, while $T >> T_0$, making $c >> v_s$.

For the 0.25-μm GaAs device at 300 K, the peak electron velocity is much greater than $v_s \approx$ 2–4 $\times 10^7$ cm/s, $c_0 = 2.7 \times 10^7$ cm/s, and the electron flow on entering the channel is again supersonic.

The transition from supersonic flow to subsonic flow in general necessitates a shock wave in gas dynamics[3]—that is, a wave over which density, velocity, and (if heat conduction equals zero) temperature change very rapidly. The n^+ drain in the source–channel–drain structure of the diode provides the mechanism that forces a supersonic flow in the channel back down to subsonic flow.

Shock waves are contained as solutions in the Boltzmann transport equation.[4] The relationship between Boltzmann and compressible fluid flow shocks then leads to the interpretation of the dramatic velocity overshoot in the DAMOCLES data as a shock wave. It is remarkable that the hydrodynamic model (which is orders of magnitude faster than Monte Carlo simulation of the Boltzmann equation) can give such excellent agreement with the DAMOCLES simulation. In addition, the hydrodynamic model provides a mathematical framework in which to understand the velocity overshoot wave.

Acknowledgment

The author wishes to thank S. Laux of the IBM Thomas J. Watson Research Center for providing the DAMOCLES results.

References

[1] C. L. Gardner, "Numerical simulation of a steady-state electron shock wave in a submicrometer semiconductor device," *IEEE Trans. Electron Devices*, vol. 38, pp. 392–398, 1991.

[2] E. Fatemi, C. L. Gardner, J. W. Jerome, S. Osher, and D. J. Rose, "Simulation of a steady-state electron shock wave in a submicron semiconductor device using high-order upwind methods," in *Computational Electronics: Semiconductor Transport and Device Simulation*. Boston, MA: Kluwer, 1991, pp. 27–32.

[3] C. L. Gardner, "Shock waves in the hydrodynamic model for semiconductor devices," in *Semiconductors* (IMA Volumes in Mathematics and its Applications). New York: Springer-Verlag, 1992.

[2]The electron temperature $T \approx$ 77 K at the shock wave. Using the effective electron mass approximation, the electron Mach number $M = v/c = v/\sqrt{T/m} \approx 2.1$.

[3]See Courant and Friedrichs [7, pp. 380–387].

[4]See Cercignani [8, pp. 369–377].

[4] M. V. Fischetti and S. E. Laux, "Monte Carlo analysis of electron transport in small semiconductor devices including band-structure and space-charge effects," *Phys. Rev. B*, vol. 38, pp. 9721-9745, 1988.
[5] G. Baccarani and M. R. Wordeman, "An investigation of steady-state velocity overshoot effects in Si and GaAs devices," *Solid-State Electron.*, vol. 28, pp. 407-416, 1985.
[6] M. V. Fischetti, "Monte Carlo simulation of transport in technologically significant semiconductors of the diamond and zinc-blende structures—Part I: Homogeneous transport," *IEEE Trans. Electron Devices*, vol. 38, pp. 634-649, 1991.
[7] R. Courant and K. O. Friedrichs, *Supersonic Flow and Shock Waves.* New York: Springer-Verlag, 1948.
[8] C. Cercignani, *The Boltzmann Equation and Its Applications.* New York: Springer-Verlag, 1988.

Current-Drive Enhancement Limited by Carrier Velocity Saturation in Deep-Submicrometer Fully Depleted SOI MOSFET's

J. G. Fossum and S. Krishnan

***Abstract*—Simulations and measurements of SOI MOSFET's are presented with analytical insight to reveal the severe limitation of current-drive enhancement caused by carrier velocity saturation in the deep-submicrometer fully depleted device. For $L = 0.1$ μm, the enhancement, which tends to result from the suppressed body charge and electric field in the thin-film device, is virtually negated by the velocity saturation driven by the high longitudinal electric field.**

I. Introduction

Thin fully depleted SOI (Si-on-SiO_2) MOSFET's offer several potential advantages over their bulk-silicon counterparts for ULSI CMOS applications [1]. One of the advantages that has been widely noted is the enhanced current drive capability of the fully depleted device [1]-[3], which is due mainly to the suppression of the body charge and transverse electric field that must be supported by the gate bias at the expense of inversion charge. This suppression tends to increase the drain saturation voltage and hence the saturation current, as well as the transconductance of the device. The same mechanism is responsible for the near-ideal subthreshold gate-voltage swing that is characteristic of the fully depleted SOI MOSFET [1].

Most of the previous analyses of the current enhancement have focused on devices with relatively long channel lengths, and have ignored the effects of carrier drift velocity saturation on channel current. Yamaguchi *et al.* [4] did present experimental data reflecting how electron velocity saturation tends to reduce the relative current enhancement as the channel length is scaled to 0.7 μm, but they provided little insight concerning shorter devices. In this brief, we emphasize deep-submicrometer devices, and show that the velocity saturation driven by the high longitudinal electric field is effective in negating the current/transconductance enhancement in the fully depleted SOI MOSFET relative to the bulk-silicon device as the channel length is scaled toward 0.1 μm. The underlying analysis uses a physical model for the SOI MOSFET [5] implemented in SOISPICE-1 [6]. The model gives good analytical insight, and simulations yield a performance benchmark of the fully depleted device relative to the bulk MOSFET for channel lengths ranging from 1.0 down to 0.1 μm. Measurements of fully depleted and non-fully depleted SOI MOSFET's, the latter of which emulates the bulk device, support the conclusion that the current-drive enhancement is limited severely by the velocity saturation, although drain-induced effects, which also depend on the body charge condition, tend to obscure the limitation.

Manuscript received June 2, 1992; revised September 21, 1992. This work was supported by the Semiconductor Research Corporation under Contract 92-SJ-273. The review of this brief was arranged by Associate Editor D. A. Antoniadis.

The authors are with the VLSI TCAD Group, Department of Electrical Engineering, University of Florida, Gainesville, FL 32611-2044.

IEEE Log Number 9205325.

II. Analysis

To put the analysis in proper perspective, we show in Fig. 1 results of dc SOISPICE-1 simulations that reflect the enhanced current drive capability of the fully depleted (TFD) n-channel SOI MOSFET with relatively long channel length ($L = 1$ μm). The basis for SOISPICE-1 is our previously developed physical model [5] for the SOI MOSFET, which allows for two modes of operation: fully depleted body with the back surface depleted (TFD), which is the mode of interest for ULSI CMOS, and fully depleted body with the back surface accumulated (TFA), which we use to model the bulk MOSFET. Indeed, when the film thickness t_b is set to the characteristic maximum depletion region width $x_{d(\max)}$, the TFA model approximates the bulk device well [7] by matching the respective body capacitances (assumed to be constant along the channel). For the TFA (bulk MOSFET) simulation of Fig. 1, the body doping was 10^{17} cm^{-3}, which defines $x_{d(\max)} \equiv t_b = 100$ nm. For the TFD simulation, the doping was 2×10^{16} cm^{-3} and $t_b = 100$ nm. For both devices, the front- and back-gate oxide thicknesses were 15 and 400 nm, respectively. To emphasize the effect of the body charge limitation on current, the (low-field) electron mobility was assigned the same value (700 cm^2/V · s) for both devices, and the same effective gate bias ($V_{GfS} - V_{Tf}$) = 1.7 V was used; the threshold voltage V_{Tf} of each device was extracted from the simulated linear-region characteristics.

The predicted saturation current of the TFD (fully depleted) device in Fig. 1 is about 50% higher than that of the TFA (bulk) device. Whereas this difference is due predominantly to the more efficient V_{GfS} control of channel charge in the TFD device because of the suppressed charge and transverse field in the body, it is influenced by drain-induced effects such as DICE (drain-induced conductivity enhancement) and channel-length modulation [5], both of which yield increasing current with increasing V_{DS}. To gain insight concerning the current enhancement, we extract from the model formalism [5] the following expression for drain current at the onset of saturation, ignoring DICE:

$$I_{DS(\mathrm{sat})} = \left(\frac{WC_{of}}{1 + \alpha}\right) \frac{m(V_{GfS} - V_{Tf})^2 v_{\mathrm{sat}}}{1 + m(V_{GfS} - V_{Tf})/(1 + \alpha)} \tag{1}$$

where $m \equiv \mu_{\mathrm{eff}}/2Lv_{\mathrm{sat}}$ with μ_{eff} being the effective electron mobility in the saturation region and v_{sat} the saturated drift velocity; and $\alpha \equiv C_b/C_{of}$ or $C_bC_{ob}/C_{of}(C_b + C_{ob})$ for TFA (bulk) or TFD, respectively, with C_{of} and C_{ob} being the front- and back-gate oxide capacitances and $C_b = \epsilon_s/t_b$ being the body (depletion) capacitance. The focus of previous commentary on the drive current enhancement [1]-[3] is on the $1/(1 + \alpha)$ proportionality of $I_{DS(\mathrm{sat})}$ in (1). Obviously α for the TFD device is smaller than that for the bulk device, which underlies the current enhancement. Physically,

0018-9383/93$03.00 © 1993 IEEE